Heliyon 10 (2024) e38041

Contents lists available at ScienceDirect

Heliyon

journal homepage: www.cell.com/heliyon

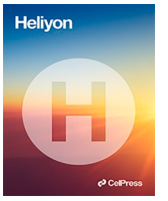

Research article

Agonist-antagonist myoneural interface surgery on the proprioceptive reconstruction of rat hind limb

Ping Wang [a,b,1], Jianping Huang [a,c,1], Jingjing Wei [a,c], Qianhengyuan Yu [a,c], Guanglin Li [a,c], Bin Yu [b], Lin Yang [a,c,**], Zhiyuan Liu [a,c,*]

[a] Shenzhen Institute of Advanced Technology of the Chinese Academy of Sciences, Shenzhen 518055, China
[b] Biomedical Sensing Engineering and Technology Research Center, Shandong University, Jinan, 25000, China
[c] University of Chinese Academy of Sciences, Beijing, 100864, China

ARTICLE INFO

Keywords:
Agonist-antagonist myoneural interface
Proprioception
Compound action potential
Nerve function repair
Muscle synergy

ABSTRACT

Currently, prosthesis users rely on visual cues to control their prosthesis. One reason for this is that prostheses cannot provide users with proprioceptive functional signals. For this reason, we propose an agonist-antagonist myoneural interface (AMI) surgery. We examined how this surgery affects the restoration of motor function and proprioceptive reconstruction in the hind limb of Sprague–Dawley rats. The procedure entails grafting the soleus muscle, suturing the two tendon ends of the soleus muscle, and anastomosing the tibial and common peroneal nerves to the soleus muscle. We found that, following surgery, AMI rats exhibited improved neurological repair, shorter walking swings, braking, propulsion, and stance times, and greater compound action potentials than control rats. This means that in rats with neurological impairment of the hind limb, the proposed AMI surgical method significantly improves postoperative walking stability and muscle synergy. AMI surgery may become an option for regaining proprioception in the lost limb.

1. Introduction

Numerous individuals experience high-energy injuries each year owing to industrial construction, and traffic accidents, natural disasters, and injuries caused by heavy object in machines and automobiles. These injuries can in turn result in neurovascular injuries, significant trauma, extensive soft tissue defects, and severe fractures. Amputation may eventually be necessary for some patients. One of the main types of prostheses used to help amputees regain limb function is the myoelectric prosthesis, which uses surface electrodes to collect nerve signals and control the movement of the prosthesis by sending cortical motor signals to the motor nerve of the limb stump according to the needs of the patient [1–6].

Kuiken et al. [7] proposed method for targeted muscle reinnervation. Simultaneously, Kung et al. [8] proposed the regenerative peripheral nerve interface (RPNI) method to enable amputees to manage their prosthesis more naturally. For prosthetic technology to

* Corresponding author. the CAS Key Laboratory of Human-Machine Intelligence-Synergy Systems, Shenzhen Institute of Advanced Technology (SIAT), Chinese Academy of Sciences (CAS), No.1068 Xueyuan Avenue, Nanshan District, Shenzhen, 518000, China.
** Corresponding author. the CAS Key Laboratory of Human-Machine Intelligence-Synergy Systems, Shenzhen Institute of Advanced Technology (SIAT), Chinese Academy of Sciences (CAS), *No.*1068 Xueyuan Avenue, Nanshan District, Shenzhen, 518000, China.
E-mail addresses: aiyzwll@aliyun.com (L. Yang), zy.liu1@siat.ac.cn (Z. Liu).
[1] Authors contributed equally as first.

https://doi.org/10.1016/j.heliyon.2024.e38041
Received 15 March 2024; Received in revised form 27 August 2024; Accepted 16 September 2024
Available online 18 September 2024

fulfill the bidirectional feedback function of the peripheral nervous system, these procedures recover the efferent signal from the transected peripheral nerve and reproduce the afferent signal buried deep in the residual tissue [9–12]. Proprioception, which includes position, motion, and vibration sensations, cannot be reconstructed because the subset of afferent signals responsible for proprioception is still notably challenging to capture in the models described above. Amputees must rely on visual cues to perform specific actions in order to compensate for their lack of profound sensation [13–15]. However, none of these systems can provide the naturally occurring neural pathways that would produce muscle-based proprioceptive functions [16].

When conscious regulatory capacity is established, proprioceptive impairment can significantly and negatively affect motor control, balance, and postural regulation [17–19]. Anterior cruciate ligament (ACL) reconstruction surgery is clinically recommended to maintain more joint ligaments in patients with hind limb knee injuries [20–23]. The ACL contains proprioceptors, such as Ruffini and Vater-Pacini, which is why this surgery is necessary. The mechanical functions of the ACL and protective and stabilizing muscle reflexes can only be engaged by maintaining more proprioceptive information [24]. Moezy et al. [25] suggested whole-body vibration training as a replacement for conventional knee training. Lin et al. [26] proposed goal-matched walking training to improve the efficacy of proprioceptive function rehabilitation by strengthening the proprioceptive feedback connections at later stages of functional reconstruction. All of the above methods are useful in helping patients with knee and ligament injuries regain their proprioception. Simple healing is insufficient for amputees who have lost all their muscles, nerves, or even joints because the loss of effectors and receptors directly disrupts the proprioceptive feedback loop.

Herr et al. [27] validated a proprioceptive construction method known as the agonist-antagonist myoneural interface (AMI) method in 2017. This method directly connects two muscle tendons in series, one representing the agonist muscle and the other the antagonist muscle, through the replication of the agonist-antagonist muscle-tendon pair. This creates a synergistic muscle relationship that maintains the stretching of the agonist muscle. Distal organs and other tissues are removed during standard amputation surgery to isotonically stabilize the remaining distal muscle tissue. This tissue is typically buried deep into the remaining limb or fatty tissue to prevent the distal end of the amputated nerve from developing phantom pain upon mechanical stimulation [28,29]. To reconstruct the proprioceptive loop system, the AMI method primarily establishes tendon connections to nearby residual muscles and directly sutures the tibialis anterior muscle to the gastrocnemius tendon. However, in patients with late amputation, the opportunity to create a muscle-tendon connection is limited due to severe muscle-tendon deficit. Pjillip et al. [30] proposed the RPNI approach, which involves the implantation of free muscle grafts to reconstruction peripheral neuromotor function in the upper extremity. In seven upper limb amputation patients, the donor muscle was chosen to be the patient's ipsilateral lateral femoral muscle, and the severed distal peripheral nerves of the upper limb residual limb were then sutured into the muscle graft to create a closed biological peripheral nerve interface. Therefore, we believe that the RPNI-based approach can be used to wrap the dissected active and antagonist nerves, based on which the tendons of the free agonist-antagonist muscles can be connected, which is more in line with the mechanism of locomotion in the physiological state. This is because the antagonist muscles are of great significance in maintaining the stability and precision of joint movement. Second, since antagonist muscles are built to modulate motor stability and coordination primarily through proprioceptive control mechanisms. Therefore, in this study, we mainly wanted to measure the proprioceptive recovery using changes in gait characteristics.

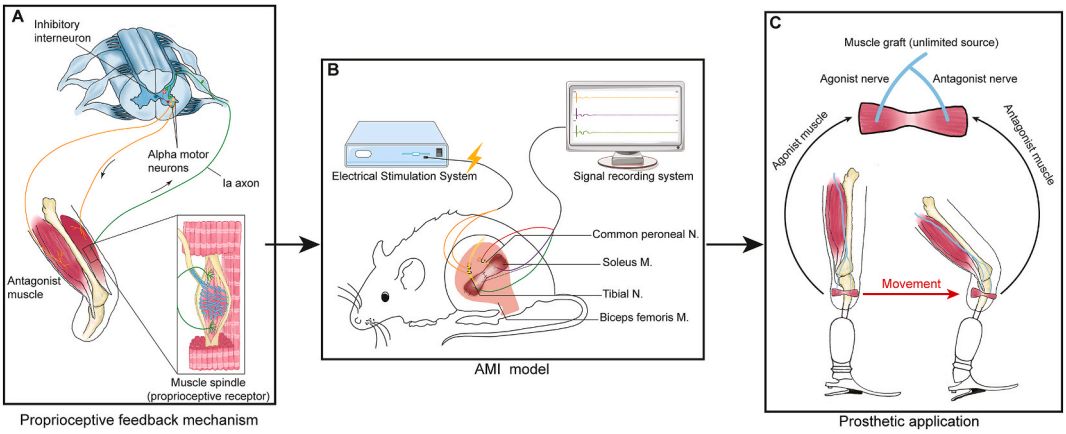

Fig. 1. AMI construction and proprioceptive reconstruction mechanism.
(A) Proprioceptive feedback mechanism: The proprioceptive pathway is mainly controlled by the cortical motor-sensory areas of the brain, with the first level of neuronal cytosol in the spinal ganglia. The muscle spindles in the skeletal muscles of the limb transmit information to the higher nervous system about the relative position and movement of muscles and joints based on the changes in the muscle length.
(B) Agonist-antagonist myoneural interface (AMI) model diagram: the soleus muscle was transplanted as the tibial and common peroneal nerve target muscles to establish an AMI model in SD rats. When the agonist muscle contracts in response to electrical stimulation, it evokes proprioceptive signals and stretches the antagonist muscles. Thus, electromyographic and neuroelectric signals can be recorded in the antagonist muscle and nerve.
(C) Prosthetic application: the AMI model offers the advantage of being suitable for patients with severe amputation and an unlimited source of donor muscles. As the anatomical relationship between the agonist and antagonist muscles is preserved in this case, it can evoke proprioceptive signals when the agonist muscle contracts. Therefore, recording the proprioceptive signals is more conducive to controlling the prosthetic actions.

This article presents a graft-targeted tendon pair strategy that expands the options for nerve implantation to the entire body. To assess the efficacy of this approach in restoring motor balance and stability in the hind limbs of rats, we constructed an AMI Sprague–Dawley (SD) rat model to analyze the changes in proprioceptive information sources and effector signals. We used the rat soleus muscle with tendons as the donor, implanted the severed tibial and common peroneal nerves in the soleus muscle belly, and anastomosed the soleus tendon end to end to form a complete anatomical closure of the nerve-muscle-tendon pair (Fig. 1). The AMI method expands upon the RPNI method by transplanting two target muscles as nerve bio-amplifiers and joining the tendons to form the fundamental motor unit. This approach has the advantage that donor muscles are readily available and the patients can choose the best donor based on their conditions. Patients can undergo a nearly unlimited degree of amputation. Moreover, this surgical method can be used if the primary functional nerve is preserved. Furthermore, as a result of the fundamental anatomical relationship stimulating the agonist-antagonist-tendon pair, the agonist muscle proprioceptors are activated when tibial nerve signaling causes the agonist muscle to contract, and the coupled antagonist muscle activates its receptors when it stretches. They then provide proprioceptive afferent signals via the common peroneal and tibial nerves. This method offers stable nerve signal transmission, making it appropriate for patients with high degrees of muscle, tendon, and nerve loss. To verify the effectiveness of this method, we created a rat amputation model using nerve dissection as a control. We then analyzed the neurologic and muscular evoked potentials post-surgery to determine whether AMI surgery could create morphological loops that directly connect the signal feedback chain. Furthermore, we investigated the mechanisms underlying proprioceptive repair using gait and histological analysis. We used the above methods to determine the nerve and muscle survival after AMI surgery and whether closed-loop feedback could effectively repair the motor balance and stability of the lower limb in rats. We aim to provide an experimental basis for the theory and technological innovation of the reconstruction of the organism's proprioceptive function after amputation, and to provide an option for patients with physical disabilities to regain the proprioception of the missing limb.

2. Materials and methods

2.1. Animal preparation

The anatomical structure, functional characteristics, and physiological responses of SD rats are similar to those of human beings. The experiments are reproducible, economically priced, and easy to feed and manage, so rats are proposed to be used as the research object in this work. Twelve male SD rats weighing 450 ± 50 g were kept in a specific pathogen-free class animal room with a temperature of (22 ± 2) °C, 40%–60 % relative humidity, and a 12 h light/dark cycle. The rats were acquired from the Guangdong Experimental Animal Center under animal permit number SCXK (Guangdong) 2017-0119. Six rats were randomly divided into AMI and control group. The Experimental Animal Ethics Committee of Shenzhen Institute of Advanced Technology, Chinese Academy of Sciences, approved the experiment (No. SIAT-IACUC-210907-JCS-HJP-A2050).

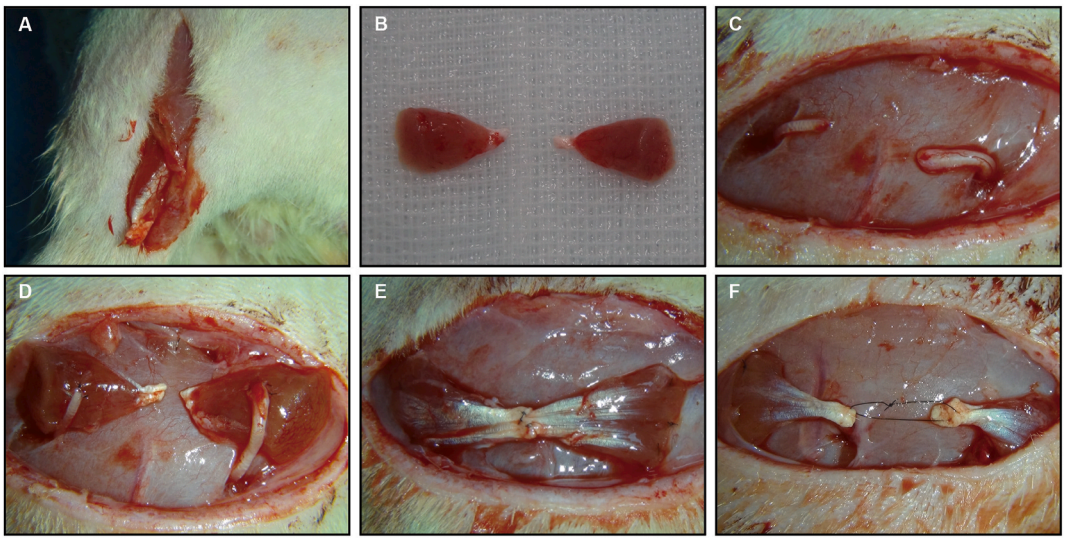

Fig. 2. Agonist-antagonist myoneural interface (AMI) and control group surgical diagram.
(A) A 1-cm incision was made along the lateral aspect of the hind limb to the Achilles tendon.
(B) The bilateral soleus muscles were removed as donor muscles.
(C) The left tibial and common peroneal nerves were dissected.
(D) The tibial and common peroneal nerves were anastomosed at the belly of the two soleus muscles.
(E) Two soleus muscles were sutured to the surface of the biceps femoris muscle membrane. The soleus muscle tendons were then anastomosed end-to-end in the AMI group.
(F) the soleus tendons were not anastomosed in the control group and were replaced with a surgical suture attachment.

2.2. Establishment of the rat model

In the AMI group, the lateral side of the left and right hind limbs of SD rats was incised 1 cm along the heel tuberosity, and general inhalation anesthesia was administered using isoflurane. The subcutaneous tissues were separated layer-by-layer, and the distal soleus tendon was liberated by carefully peeling off the fascia and connective tissues surrounding the tendons of the distal extremities of the two muscles. After removing the residual blood, the excised graft was promptly washed in a sodium heparin solution (400 units/mL) and submerged in saline. Subsequently, the common tibial and peroneal nerves were divided and detached distally, and their proximal ends were inserted at the belly of the two soleus muscles using a 12-0 suture. A 6-0 suture was used to end-anastomose the two soleus tendons, and a 8-0 sutures were used to implant the soleus muscle at the surface fascia of the biceps femoris. They were then sutured layer by layer onto the skin. The blood supply to the graft is provided by the donor muscle. Free soleus muscle sutured to the surface of the biceps femoris muscle reconstruction the blood supply to the muscle and provides access to the nerves and tendons, ensuring the survival of the nerves, muscles and tendons after AMI.

In the control group, two soleus muscles were implanted at the biceps femoris muscle membrane, after which, the two muscles were only penetrated and slightly fixed with 6-0 suture, and the two tendons were not anastomosed. Muscle grafting and nerve implantation were performed as described for the AMI group (see Fig. 2).

2.3. Gait analysis

The postoperative footprints and gait of the rats were recorded using a gait analysis system (BT60101; Shenzhen Zhongshi Company, China). The system was outfitted with a 1/4" CCD high-speed camera featuring a 640 × 480 lens resolution, ultra-low illumination (0.05 1X), 120 frames per second, and a cold light source. This device monitored the soles of the feet with a camera using the footprint light refraction technique to determine the walking gait of the animal.

The distances between the heel and tip of the foot, first and fifth toes, and second and fourth toes were measured from three complete footprints taken from the operated side and three from the non-operated side. The sciatic nerve function index (SFI), tibial nerve function index (TFI), and standard peroneal nerve function index (PFI) were computed by substituting the abovementioned measurements the Bain's method:

SFI = −38.3 × [(operative PL − healthy PL)/healthy] + 109.5 × [(operative TS − healthy TS)/healthy TS] + 13.3 [(operative ITS − healthy ITS)/healthy ITS] − 8.8, TFI = −37.2 × [(operative side PL − healthy side PL)/healthy side] + 104.4 × [(operative side TS − healthy side TS)/healthy side TS] + 45.6 [(operative side ITS − healthy side ITS)/healthy side ITS] − 8.8, PFI = −174.9 × [(operative PL − healthy PL)/healthy] + 80.3 × [(operative TS − healthy TS)/healthy TS] + 13.3 [(operative ITS − healthy ITS)/healthy ITS] − 13.4,PL, heel-to-toe distance of each hindfoot; TS, distance from the first toe to the fifth toe of the hindfoot; ITS, distance from the second toe to the fourth toe of the hind foot.

One of the primary indices used to evaluate the restoration of neurological function after surgery in rats is the neurological function index. Additional statistics were synchronized to the paw angle (PA), vector, paw angle-body angle (PABA), measurement of walking swing duration, braking duration, propulsion duration, stance duration, and average pressure-contact intensity of the hind foot:

Walking swing duration = time maintained before plantar contact with the running platform.

Braking duration = duration from plantar contact with the running platform to the maximum contact surface of the plantar foot with the running platform.

Propulsion duration = duration from the maximum contact area between the plantar foot and running platform to the duration of platform exit.

Stance duration = entire duration of plantar contact with the running platform.

The average pressure-contact intensity of the hindfoot is reflected by the optical density ratio after contact between the sole and running platform.

2.4. Characteristics of electromyographic signals and neuroelectrical information

Hook-shaped microelectrodes (stainless steel, 0.25 mm diameter) were positioned at the tibial and common peroneal nerves, respectively, and the Plexstim stimulator (OPX-D2; Plexon, USA) provided stimulation signals with varying 50 μs pulse width and 1 Hz frequency. When a signal is received for a given stimulus, it is customary, to begin with no target muscle contraction and progressively increase the signal as the stimulus enhancement becomes more intense until the target muscle contraction remains unchanged. After the stimulus is repeated, the intensity IS = IA × (1 + 20 %) is recorded as the initial stimulus intensity, or IA. The microelectrodes (stainless steel, 0.25 mm diameter) collected the corresponding tibial nerve and common peroneal nerve compound nerve action potential (CNAP),compound muscle action potential (CMAP) of the tibial nerve innervated graft and the CNAP of the standard peroneal nerve graft. The latency (t) is the amount of time that passes between stimulation artifacts and evoked potentials. The distance (s) between the stimulating electrode and each recording electrode (tibial nerve to the left soleus muscle and common peroneal nerve to the right soleus muscle) was measured. It was determined that the motor nerve conduction velocity (MCV) was MCV = s/t. The CMAP and CNAP were pre-processed by filtering and noise reduction to extract the signals in the influential frequency domain band, and the Omniplex system software, provided by Plexon was used to handle the raw signals. After feature configuration, the signal bands corresponding to the sensory stimuli were acquired, and the spectra and peaks were further produced. It was established that stimulus-muscle and nerve signals corresponded to each other.

2.5. Body and muscle wet weights

The gastrocnemius, tibialis anterior, and graft tendons were removed after anesthesia and weighed two months after surgery. The body weights of the rats in the two groups were also recorded before and two months after surgery.

2.6. Histological staining

Rat muscle-tendon pairs were extracted, clipped, and fixed in 4 % formaldehyde solution. After staining, the sections were regularly sectioned to a thickness of 5 μm, sequentially transparent, dehydrated, paraffin-embedded, and sealed with a neutral resin. The skin morphology and pathological alterations were examined under a microscope. The distribution and constructive characteristics of muscle spindles and tendons in the target tissues were observed using hematoxylin and eosin (HE) staining (BH0001; Boerfu Biotechnology, Inc., China), with particular attention paid to the morphology of muscle myocytes, number and morphology of tendons and spindles, growth of blood vessels, and healing of anastomosis. The degree of tendon fibrosis was observed using Masson staining (BH0002; Boerfu Biotechnology, Inc., China).

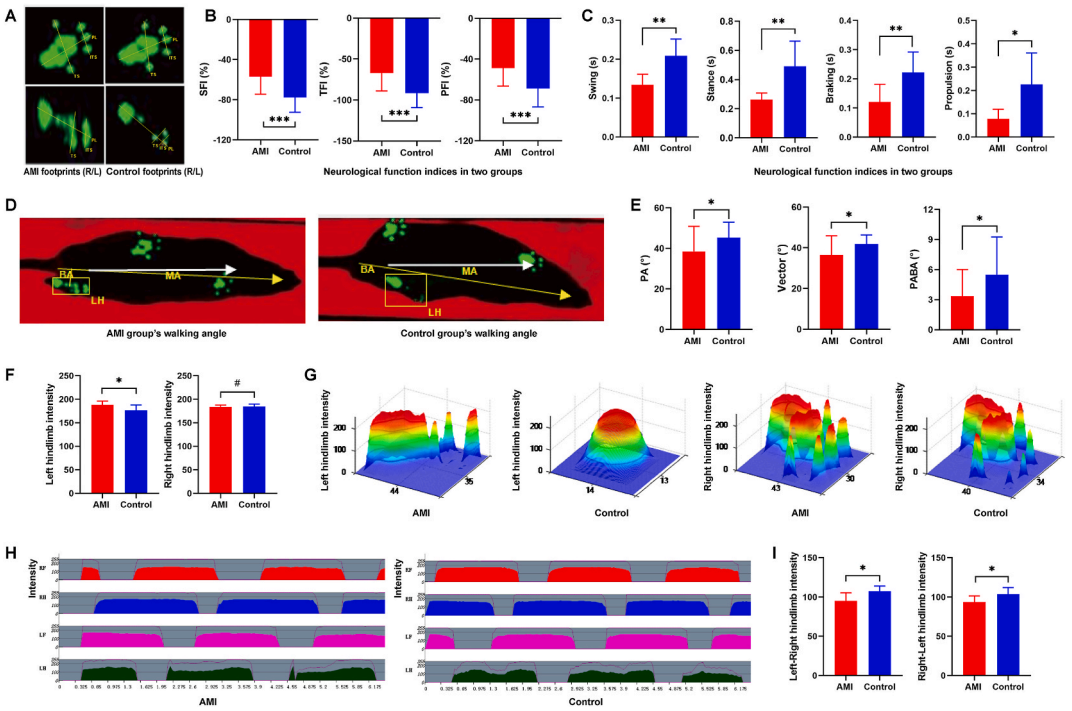

Fig. 3. Gait analysis data after surgery.
(A) The atrophy of the left foot (lower panel) in the AMI group compared to the right foot (upper panel) was evident, while the atrophy in the control group was more severe.
(B) The absolute values of SFI, TFI, and PFI in the AMI group (red) were significantly smaller than those in the control group (blue). This indicates that the postoperative motor functions of the sciatic, tibial and common peroneal nerves of the rats in the AMI group were superior to those of the control group.
(C) The duration of walking, swinging, braking, propulsion, and stance of the rats in the AMI group (red) were all smaller than those in the control group (blue). This indicates that the rats in the AMI group moved faster than the control group during walking and had better control of all stages of walking than the control group.
(D) The angle between the walking direction and the rat body position in the AMI group was minor, while that in the control group was more deviated toward the affected foot. This indicates that AMI rats have better body balance during walking than the control group.
(E) The PA, vector, and PABA of the rats in the AMI group (red) were smaller than those in the control group (blue). This suggests that the control rats that did not undergo AMI surgery during walking mainly increased the left hind walking angle to control body balance.
(F) The pressure intensity of the left foot in contact with the flat surface of the rats in the AMI group was less than that in the control group, and the right foot did not show statistically different outcomes from the control group.
(G) The contact area and pressure of the plantar surface of the left limb of the rats in the AMI group were slightly weaker than those of the right side, while the contact area of the plantar surface of the affected limb of the control group was very small.
(H) The pressure of the left limb in the AMI group was unstable during walking, showing only brief lifting movements, while the control group showed a continuous decrease in pressure.
(I) The mean pressure-touch intensity of the AMI group's left-to-right and right-to-left walking process was less than that in the control group.

2.7. Statistical analysis

The measurement results of statistical analysis, including the SFI, TFI, PFI, were represented as mean ± standard deviation. Repeated measurements were performed using the Statistical Package for Social Sciences software (version 22.0). The repeated

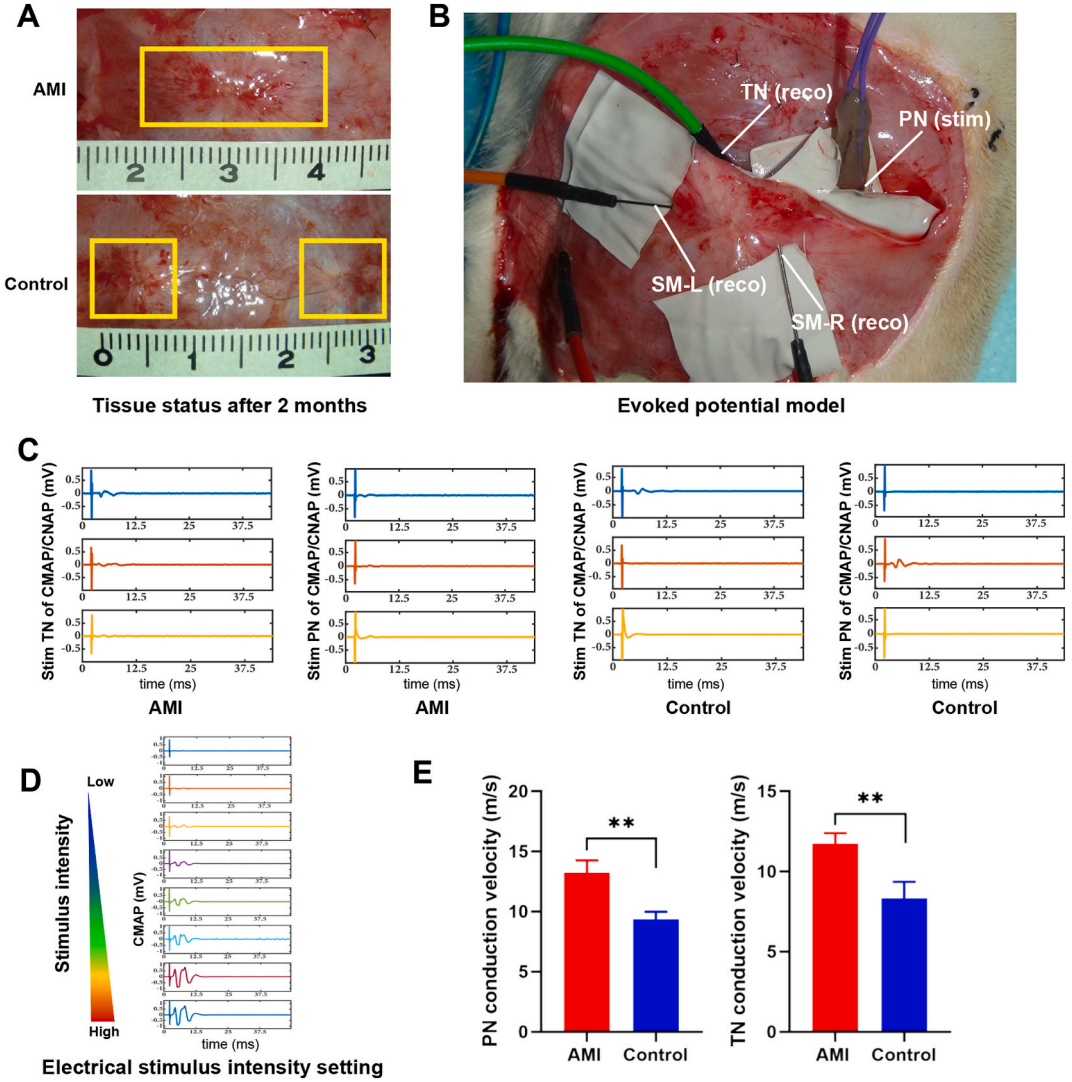

Fig. 4. Signal analysis.
(A) State of graft repair in both the groups of rats at 2 months postoperatively.
(B) Electrical stimulation of the tibial nerve (agonist), recording of CMAP (agonist-antagonist myoneural) in the soleus muscle, and CNAP (antagonist) in the common peroneal nerve. It can be seen that the two grafts in the AMI group were connected together, while the control group grafts were spaced far apart from each other.
(C) On stimulation of the tibial nerve in the AMI group, CMAP of the tibial nerve (blue) and common peroneal nerve (red) innervated side grafts and CNAP of common peroneal nerve (orange) could be collected. On the stimulation of the common peroneal nerve in the AMI group, CMAP of common peroneal nerve (blue) and tibial nerve (red) innervated side grafts and CNAP of common peroneal nerve (orange) could be collected. Only CMAP for tibial nerve (blue) innervated side grafts could be recorded on the stimulation of the tibial nerve in the control group. CMAP of the common peroneal nerve innervated side grafts (red) and CNAP of the common peroneal nerve (orange) could not be evoked. Only CMAP of the common peroneal nerve (blue) innervated lateral grafts were collected on the control common peroneal nerve stimulation. CMAP of the tibial nerve innervated lateral grafts (red), and CNAP of the tibial nerve (orange) were not evoked. The above results indicate that when the active nerve was stimulated, both the antagonist muscle and the nerve could be evoked in the AMI group, whereas in the control group, only the active muscle wrapping the nerve could be evoked, and neither the antagonist muscle nor the antagonist nerve could be evoked.
(D) Gradual increase in the stimulation intensity to evoke CMAP/CNAP. (E) Both tibial and common peroneal nerve conduction velocities were higher in the AMI group than in the control group. It indicates that the repair effect of neuromotor function in the AMI group was better than that in the control group.

measures ANOVE test were assessed using analysis of variance. Intra-group comparison was made using the least significant difference-t test. The differences between the two groups that shared the same index were examined using the independent sample *t*-test. Normalcy transformation was necessary when the measurement data did not fit the expected distribution; and the differences were examined usingan $\alpha = 0.05$ test. To account for two comparisons of different groups, the test was modified as follows: $\alpha' = \alpha/k \times (k - 1)/2$.

3. Results

3.1. Tendon anastomosis facilitates gait stability in rats

The AMI group showed significantly less functional deficit, as indicated by the SFI, TFI, and PFI, as well as the PA, vector, the PABA of the gait angle values two months after surgery. These differences were considered statistically significant ($P < 0.05$). There was a significant difference ($P < 0.05$) in the walking swing, braking, propulsion, and stance durations between the AMI and control groups. The left hind-foot in both groups had a lower mean pressure-touch intensity than that in the control group. In addition, the left-to-right walking process in the AMI group had a lower pressure-touch intensity than that in the control group. These differences were statistically significant ($P < 0.05$), as shown in Fig. 3, Supplementary 1, 2.

3.2. The higher amplitude of evoked CMAP & CNAP indicates better neuronal remodeling and muscle repair

In the AMI group, the CMAP of the graft on the innervated side of the common peroneal and tibial nerves, and CNAP of the tibial nerve were all stronger when the left common peroneal nerve was stimulated. Additionally, the CMAP of the graft and the CNAP of the tibial nerve were gradually enhanced as the stimulation intensity increased (Fig. 4, Supplementary 3, 4). The AMI group collected the CMAP of the graft on the innervated side of the peroneal and tibial nerves, and CNAP of the peroneal nerve. In the control group, only the CMAP of the graft on the innervated side of the peroneal nerve was recorded. Grafts on the innervated side of the tibial nerve and their CNAP could not be recorded. Three points were selected and stimulated independently to determine the conduction velocities of the tibial and common peroneal nerves. The time interval between the evoked potentials and stimulation artifacts were recorded. As shown in Fig. 4, Supplementary 5,6, 7 we found that the AMI group had faster peroneal and tibial nerve conduction velocities than the control group. This difference was statistically significant ($P < 0.05$).

3.3. Loss of innervation leads to severe atrophy of muscle and tendon tissues

The differences in body weight, graft mass, and tibialis anterior and gastrocnemius muscle mass between the left and right hind limbs of rats in both groups prior to and two months after following surgery were not statistically significant ($P > 0.05$). However, Table 1 illustrates that the tibialis anterior and gastrocnemius muscle masses of the right hind limb were significantly higher than those of the left hind limb in both groups, and the differences were statistically significant ($P < 0.05$).

3.4. Re-establishment of the innervation and formation of closed-loop anatomy facilitates tissue repair

The HE staining results showed that the tendon pairs in the AMI group healed entirely and were connected. However, some muscles in this group showed atrophy with few standard muscle spindles. Likewise, the tendons and muscles in the control group showed atrophy and a loss of normal morphology and structure. Collagen fibers in the tendons of the AMI group were structurally intact, whereas those in the control group were dispersed and fragmented (Fig. 5).

4. Discussion

Human limbs possess a sophisticated sensory system as well as robust and flexible motor functions. Proprioceptive receptors in muscles, tendons, and joints regulate limb position and movement accuracy through position, kinesthetic, and vibration senses [31, 32]. In contrast, fingertips use superficial senses such as touch pressure to perceive information about the surrounding environment and issue commands to control limb activities. Nevertheless, amputees who use conventional prostheses cannot sense their

Table 1
Comparison of body weight and muscle weight between two groups of rats (g).

Group	*n*	Weight	Graft mass	TAM(L)	TAM(R)	GAM(L)	GAM(R)
AMI group	8	615.50 ± 56.26	0.13 ± 0.08	0.25 ± 0.04	1.12 ± 0.11*	0.79 ± 0.15	3.95 ± 0.29*
Control group	6	581.83 ± 61.33	0.15 ± 0.03	0.22 ± 0.06	1.07 ± 0.06*	0.78 ± 0.16	3.64 ± 0.38*
t		1.067	0.578	1.126	1.001	0.120	1.737
P		0.307	0.574	0.282	0.337	0.906	0.108

Note: *P < 0.05 compared to the left. TAM(L) indicates the tibialis anterior muscle of the left hind limb. TAM(R) indicates the tibialis anterior muscle of the right hind limb. GAM(L) indicates the gastrocnemius muscle of the left hind limb. GAM(R) indicates the gastrocnemius muscle of the right hind limb.

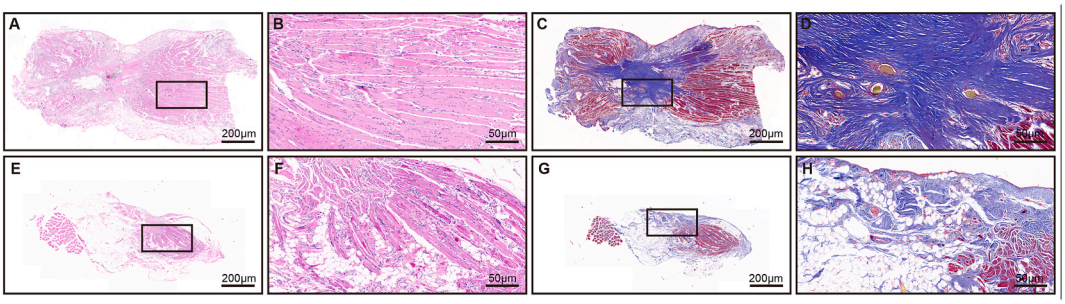

Fig. 5. Histological staining.
(A) HE staining of the AMI group (2X): soleus muscle-tendon pairs.
(B) HE staining of the AMI group (10X): partial muscle atrophy with essentially intact structure.
(C) Masson staining of the AMI group (2X): soleus muscle-tendon pair.
(D) Masson staining of the AMI group (10X): complete healing of the soleus muscle-tendon pair with the intact connection.
(E) HE staining of the control group (2X): single soleus muscle.
(F) HE staining of the control group (10X): severe muscle atrophy with the loss of normal tissue structure.
(G) Masson staining of the control group (2X): single soleus muscle.
(H) Masson staining of the control group (10X): complete atrophy of the tendon, severe fattening, and structural disorder.

environment, perform precise movement commands, or perceive the position, speed, and direction of motion of the prosthesis in the same manner as they would in a normal limb [33].

There are two types of proprioceptive dominance modalities: conscious and nonconscious. The motor sensory areas integrated in the brain cortex control the conscious proprioceptive pathway [34]. Unconscious proprioception features conditioned reflex mode (low level) and motor regulation of muscles and joints by the cerebellum and vestibule (intermediate level) [35]. Although a highly focused motor intent from the user is crucial for controlling a prosthetic limb, a person typically uses a combination of conscious and unconscious pathways to operate their limbs [36]. More trunk balance, postural adjustment, and motor control are needed for lower limb control than for upper limb control. However, owing to the loss of proprioceptive receptors or the absence of limb muscles and tendons, patients with lower limb amputation experience a severe lack of sensory information while processing limb position and spatial movement [37–41]. To compensate for this, we reconstructed the proprioceptive pathway by optimizing the conscious pathway and fixing the unconsciously controlled anatomical pathway.

What, therefore, is the secret that helps amputees of lower limbs regain their proprioception? The goal is to rebuild the closed-loop structure between the receptor, afferent nerve, center, efferent nerve, and effector or to strengthen the feedback function of the initially lost proprioceptors. First, the fast-transmitting afferent feedback dispersed throughout the skeletal muscle of the limb predominantly encodes the analysis of muscle length signal and muscle extension changes. It then modulates the joint mobility during postural control in response to the extension reflex. However, the afferent input of kinesthetic information is significant for limb movement phase and pattern switching, and the tendon spindle senses changes in limb weight-bearing to assist the with pedestrian motor load control to move the limb forward [42–44]. This delicate pattern of muscle movement regulation informs the higher nervous system about the relative position and movement of relevant muscles and joints. In prosthetic patients, the absence of tissues, including muscles and joints, results in the loss of receptors and effectors, directly disrupting the reflex loop [45]. Second, walking is not unconscious; instead, it involves “low-level” regulation of muscle and tendon spindle receptors and “high-level” cognitive control. This makes walking significantly more difficult for prosthesis users in terms of motor executive function and attentional control [46].

Herr et al. tandemly coupled the gastrocnemius-anterior tibialis muscle in mice to determine the fundamental anatomical relationship of the agonist-antagonist myoneural. The agonist muscle was contracted using an external device to activate the agonist proprioceptive receptors on the efferent nerve. Meanwhile, the antagonist’s muscle was stretched in tandem to activate its receptors, producing proprioceptive afferent signals via the tibial and common peroneal nerves [47–50]. The AMI method restores deep sensory functions, such as motion position and vibration perception in the limb to provide amputees with natural limb sensation by reestablishing this fundamental motor synergy between the agonist-antagonist myoneural pair. It also uses existing flexible interface technologies and physiologically relevant proprioceptive feedback from biological neural pathways to convert prosthetic sensory information related to muscle stretching and tension into neural signals. Thus, by developing a successful method for reconstructing the proprioceptive function in the missing limb using an animal model of limb disability, we examined the effects of proprioceptive rehabilitation in rats following AMI surgery.

In this study, we used a microscopic nerve anastomosis method to create a rat model in which the tibial and common peroneal nerves of the left hind limb were disarticulated. This study addressed the loss of limb proprioceptive function caused by disruption of the connection between proprioceptive signals and receptors after amputation. The ventral aspect of the soleus muscles was grafted, the severed nerve was anastomosed to the ventral aspect of the soleus muscles, and the grafted tendon was anastomosed to complete AMI surgery. The postoperative muscle synergistic effects in the rats were assessed using electrophysiological methods, gait analysis, and the expression of TIMP-1 and MMP-1 in the tendon during a two-month repair period. These indicators confirmed the efficacy of the proposed model. The gastrocnemius and tibialis anterior muscles in the AMI group (tendon anastomosis) and control group (tendon

dissection) exhibited significant atrophy compared to the healthy side (right side) of the body, and the degree of atrophy did not differ significantly between both groups. Two months after surgery, the gait balance ability and repair status of the injured nerve function in the AMI group appeared to be better than those in the control group, as evidenced by the significantly lower absolute values of SFI, TFI, and PFI, as well as the values of PA, vector, and PABA.

We have always emphasized the importance of proprioception, but it is very difficult for us to directly detect proprioception in animals. Simply put, each of us can feel the speed and angle of movement of our own limbs, but no one else can. One of the important roles of proprioception is to maintain motor stability and limb balance by antagonizing the muscles, so we indirectly evaluated the recovery of proprioception after surgery by observing the movement control ability and the angle of limb movement during the walking process. The amount of time spent walking before the hind limb touches the ground is known as the walking swing duration, which is generally shorter when the pace at which one walks is faster. A lack of kinesthesia and position sensation extends the swing duration before the hind limb touches the ground [51]. Pain and hind limb motor function limitations caused by muscle and joint illnesses can also prolong the swing duration. When the limb reaches the stage of deceleration and control of the standing posture, the hind limb begins to contact the ground following the swing phase. This is the period during which the hind limb braking. The delay at this stage could indicate that the body requires more time to distribute and regulate the standing load evenly to maintain limb balance. The distance between the maximum contact area of the rear foot with the ground and the next swing phase is known as the propulsion duration; that is, this is the time required to continue the forward motion. The shortened duration of this accelerated movement suggests increased trunk strength and control [52]. The entire period of rear foot-ground contact is known as the stance duration, and it often has a positive correlation with walking speed. Many influencing factors are related to hind limb-ground contact intensity, and the rat body weight, plantar area, ground friction, motor status, and limb control can all change the contact intensity [53]. Herr's team primarily illustrated the signal feedback loop problem through muscle force-electrical signal correlation.

The results of this study demonstrate that the rats that underwent AMI surgery presented significantly shorter walking swing, braking, propulsion, and stance durations than those underwent tendon dissection after two months. This means that the hind limb motor control of the rats could be restored through the intact neurofeedback loop created by AMI.

According to the stimulation-evoked electrical signal experiment, the CMAP signal of the peroneal nerve innervated graft (agonist muscle) gradually strengthened with higher stimulation of the common peroneal nerve (agonist nerve) in rats that underwent AMI. Simultaneously, there was an increase in the CMAP signal of the tibial nerve (antagonist nerve) and an enhancement of the CNAP signal of the tibial nerve innervated graft (antagonist nerve). The antagonist muscle and antagonist nerve of the control group with the severed tendon presented no evident feedback effect on the stimulation signal, and the results showed that the co-motor unit of the muscle-tendon pair-nerve could form a closed loop to complete the feedback of afferent and efferent signals. The rats in the AMI group featured faster conduction velocities for both the tibial and common peroneal nerves than those in the control group. This suggests that following AMI surgery, the agonist and antagonist muscles of the hind limb had a positive synergistic effect, and that the motor function of the injured nerve had significantly recovered.

The tibial and common peroneal nerves in rats can be restored to function in the hind limb by transplanting normal muscle tendons from other parts to create an agonist-antagonist myoneural basic motor unit. This method can significantly improve postoperative motor stability and muscle synergy in rats, and overcome the previous restriction that dissociated nerve implantation can only select nearby target organs without affecting electromyography, electroencephalogram collection, and extraction. However, this study has some limitations. First, this study used an animal model, and the sample size is limited, so the practical application value is insufficient, and the applicability of this approach to amputation patients' needs to be further verified by clinical trials. Second, it was not possible to precisely separate individual proprioceptive signals from composite ENG signals for reference, and it was not possible to examine the impact of this model on the innervation of the cerebral sensory cortex. Third, this study did not explore all proprioceptive receptors, including those in the tendons and muscle spindles. Fourth, considering the complex construction process of this model and gradual healing of tendons, further research is required to determine whether drugs, and thermal, electrical, and motor stimulations can aid in rehabilitating the hind limb motor function.

Funding

This work was supported in part by Strategic Priority Research Program of the Chinese Academy of Sciences (#XDB0930000) , and the National Key Scientific Instrument and Equipment Development Projects of China (#Y920921001), and Key Technologies Research and Development Program (#2021YFF0501601), and Innovative Research Group Project of the National Natural Science Foundation of China (#82260456, #81960419), and Shandong University Integrated Tackling Cultivation Program (#2022JC004).

Data availability

Data will be made available on request.

CRediT authorship contribution statement

Ping Wang: Writing – original draft, Visualization, Software, Methodology, Investigation, Formal analysis. **Jianping Huang:** Writing – original draft, Visualization, Software, Methodology, Investigation, Formal analysis. **Jingjing Wei:** Software, Investigation, Formal analysis. **Qianhengyuan Yu:** Visualization, Project administration, Investigation. **Guanglin Li:** Writing – review & editing, Supervision, Project administration, Funding acquisition. **Bin Yu:** Writing – review & editing, Validation, Supervision. **Lin Yang:**

Writing – review & editing, Validation, Supervision, Project administration, Funding acquisition, Conceptualization. **Zhiyuan Liu:** Writing – review & editing, Validation, Supervision, Resources, Project administration, Funding acquisition, Data curation, Conceptualization.

Declaration of competing interest

There is no conflict of interest regarding the publication of this paper.

Acknowledgments

We thank PhD. Shengyong Ding for technical assistance of this work.

Appendix A. Supplementary data

Supplementary data to this article can be found online at https://doi.org/10.1016/j.heliyon.2024.e38041.

References

[1] N. Parajuli, N. Sreenivasan, P. Bifulco, et al., Real-time EMG based pattern recognition control for hand prostheses: a review on existing methods, challenges and future implementation, Sensors 19 (20) (2020) 4596, https://doi.org/10.3390/s19204596.
[2] C. Antfolk, M. D'Alonzo, B. Rosen, et al., Sensory feedback in upper limb prosthetics, Expet Rev. Med. Dev. 10 (1) (2013) 45–54, https://doi.org/10.1586/erd.12.68.
[3] L. Foroni, M.G. Siqueira, R.S. Martins, G.P. Oliveira, The intercostobrachial nerve as a sensory donor for hand reinnervation in brachial plexus reconstruction is a feasible technique and may be useful for restoring sensation, Arq Neuropsiquiatr 75 (7) (2017) 439–445, https://doi.org/10.1590/0004-282X20170073.
[4] E. D'Anna, F.M. Petrini, F. Artoni, I. Popovic, I. Simanic, S. Raspopovic, S. Micera, A somatotopic bidirectional hand prosthesis with transcutaneous electrical nerve stimulation based sensory feedback, Sci. Rep. 7 (1) (2017) 10930, https://doi.org/10.1038/s41598-017-11306-w.
[5] L. Foroni, M.G. Siqueira, R.S. Martins, C.O. Heise, H.N. Sterman, A.Y. Imamura, Good sensory recovery of the hand in brachial plexus surgery using the intercostobrachial nerve as the donor, Arq Neuropsiquiatr 75 (11) (2017) 796–800, https://doi.org/10.1590/0004-282X20170148.
[6] M. Schiefer, D. Tan, S.M. Sidek, D.J. Tyler, Sensory feedback by peripheral nerve stimulation improves task performance in individuals with upper limb loss using a myoelectric prosthesis, J. Neural. Eng. 13 (1) (2016) 016001, https://doi.org/10.1088/1741-2560/13/1/016001.
[7] T.A. Kuiken, L.A. Miller, R.D. Lipschutz, B.A. Lock, K. Stubblefield, P.D. Marasco, P. Zhou, G.A. Dumanian, Targeted reinnervation for enhanced prosthetic arm function in a woman with a proximal amputation: a case study, Lancet 369 (9559) (2007) 371–380, https://doi.org/10.1016/S0140-6736(07)60193-7.
[8] T.A. Kung, N.B. Langhals, D.C. Martin, P.J. Johnson, P.S. Cederna, M.G. Urbanchek, Regenerative peripheral nerve interface viability and signal transduction with an implanted electrode, Plast. Reconstr. Surg. 133 (6) (2014) 1380–1394, https://doi.org/10.1097/PRS.0000000000000168.
[9] Z.T. Irwin, K.E. Schroeder, P.P. Vu, D.M. Tat, A.J. Bullard, S.L. Woo, I.C. Sando, M.G. Urbanchek, P.S. Cederna, C.A. Chestek, Chronic recording of hand prosthesis control signals via a regenerative peripheral nerve interface in a rhesus macaque, J. Neural. Eng. 13 (4) (2016) 046007, https://doi.org/10.1088/1741-2560/13/4/046007.
[10] W.C. Lineaweaver, F. Zhang, Clarifying the role of targeted muscle reinnervation in amputation management, J. Am. Coll. Surg. 229 (6) (2019) 635, https://doi.org/10.1016/j.jamcollsurg.2019.08.1444.
[11] F. Mereu, F. Leone, C. Gentile, F. Cordella, E. Gruppioni, L. Zollo, Control strategies and performance assessment of upper-limb tmr prostheses: a review, Sensors 21 (6) (2021) 1953, https://doi.org/10.3390/s21061953.
[12] T.A.M.P. Kuiken, B.A. Lock, R.N. Harden, J.P. Dewald, Redirection of cutaneous sensation from the hand to the chest skin of human amputees with targeted reinnervation, Proc. Natl. Acad. Sci. U.S.A. 104 (2021) 6, https://doi.org/10.1073/pnas.0706525104.
[13] A.S. Dhawan, B. Mukherjee, S. Patwardhan, N. Akhlaghi, G. Diao, G. Levay, R. Holley, W.M. Joiner, M. Harris-Love, S. Sikdar, Proprioceptive Sonomyographic Control: a novel method for intuitive and proportional control of multiple degrees-of-freedom for individuals with upper extremity limb loss, Sci. Rep. 9 (1) (2019) 9499, https://doi.org/10.1038/s41598-019-45459-7.
[14] S. Sundaram, P. Kellnhofer, Y. Li, J.Y. Zhu, A. Torralba, W. Matusik, Learning the signatures of the human grasp using a scalable tactile glove, Nature 569 (7758) (2019) 698–702, https://doi.org/10.1038/s41586-019-1234-z.
[15] B.M. Sexton, Y. Liu, H.J. Block, Increase in weighting of vision vs. proprioception associated with force field adaptation, Sci. Rep. 9 (1) (2019) 10167, https://doi.org/10.1038/s41598-019-46625-7.
[16] M. Rossi, M. Bianchi, E. Battaglia, M.G. Catalano, A. Bicchi, HapPro: a wearable haptic device for proprioceptive feedback, IEEE Trans. Biomed. Eng. 66 (1) (2019) 138–149, https://doi.org/10.1109/TBME.2018.2836672.
[17] N. Elangovan, L. Cappello, L. Masia, J. Aman, J. Konczak, A robot-aided visuo-motor training that improves proprioception and spatial accuracy of untrained movement, Sci. Rep. 7 (1) (2017) 17054, https://doi.org/10.1038/s41598-017-16704-8.
[18] G.J. Kavounoudias A, R. Roll, J.P. Roll, From balance regulation to body orientation: two goals for muscle proprioceptive information processing, Exp. Brain Res. 124 (1999) 9, https://doi.org/10.1007/s002210050602.
[19] C. Landelle, J.L. Anton, B. Nazarian, J. Sein, A. Gharbi, O. Felician, A. Kavounoudias, Functional brain changes in the elderly for the perception of hand movements: a greater impairment occurs in proprioception than touch, Neuroimage 220 (2020) 117056, https://doi.org/10.1016/j.neuroimage.2020.117056.
[20] A. Prodromidis, N. Zreik, G. Thivaios, A. Waqar, P. Dey, C. Charalambous, Relationship of timing of anterior cruciate ligament (ACL) reconstruction surgery with meniscal tears, chondral injuries, functional and patient reported outcomes. A systematic review, Int. J. Surg. 47 (2017) S77, https://doi.org/10.3389/fphys.2020.00090.
[21] R. Thomee, Y. Kaplan, J. Kvist, G. Myklebust, M.A. Risberg, D. Theisen, E. Tsepis, S. Werner, B. Wondrasch, E. Witvrouw, Muscle strength and hop performance criteria prior to return to sports after ACL reconstruction, Knee Surg. Sports Traumatol. Arthrosc. 19 (11) (2011) 1798–1805, https://doi.org/10.1007/s00167-011-1669-8.
[22] C.L. Ardern, N.F. Taylor, J.A. Feller, K.E. Webster, Return-to-sport outcomes at 2 to 7 years after anterior cruciate ligament reconstruction surgery, Am. J. Sports Med. 40 (1) (2012) 41–48, https://doi.org/10.1177/0363546511422999.
[23] B. Noehren, A. Abraham, M. Curry, D. Johnson, M.L. Ireland, Evaluation of proximal joint kinematics and muscle strength following ACL reconstruction surgery in female athletes, J. Orthop. Res. 32 (10) (2014) 1305–1310, https://doi.org/10.1002/jor.22678.
[24] F.H. Co, H.B. Skinner, W.D. Cannon, Effect of reconstruction of the anterior cruciate ligament on proprioception of the knee and the heel strike transient, J. Orthop. Res. 11 (5) (1993) 696–704, https://doi.org/10.1002/jor.1100110512.

[25] A. Moezy, G. Olyaei, M. Hadian, M. Razi, S. Faghihzadeh, A comparative study of whole body vibration training and conventional training on knee proprioception and postural stability after anterior cruciate ligament reconstruction, Br. J. Sports Med. 42 (5) (2008) 373–378, https://doi.org/10.1136/bjsm.2007.038554.
[26] D.H. Lin, C.H. Lin, Y.F. Lin, M.H. Jan, Efficacy of 2 non-weight-bearing interventions, proprioception training versus strength training, for patients with knee osteoarthritis: a randomized clinical trial, J. Orthop. Sports Phys. Ther. 39 (6) (2009) 450–457, https://doi.org/10.2519/jospt.2009.2923.
[27] T.R. Clites, M.J. Carty, S. Srinivasan, A.N. Zorzos, H.M. Herr, A murine model of a novel surgical architecture for proprioceptive muscle feedback and its potential application to control of advanced limb prostheses, J. Neural. Eng. 14 (3) (2017) 036002, https://doi.org/10.1088/1741-2552/aa614b.
[28] G.M. Hobusch, K. Doring, R. Branemark, R. Windhager, Advanced techniques in amputation surgery and prosthetic technology in the lower extremity, EFORT Open Rev 5 (10) (2020) 724–741, https://doi.org/10.1302/2058-5241.5.190070.
[29] A. Chopra, A.F. Azarbal, E. Jung, C.Z. Abraham, T.K. Liem, G.J. Landry, G.L. Moneta, E.L. Mitchell, Ambulation and functional outcome after major lower extremity amputation, J. Vasc. Surg. 67 (5) (2018) 1521–1529, https://doi.org/10.1016/j.jvs.2017.10.051.
[30] P.P. Vu, A.K. Vaskov, Z.T. Irwin, P.T. Henning, D.R. Lueders, A.T. Laidlaw, A.J. Davis, C.S. Nu, D.H. Gates, R.B. Gillespie, S.W.P. Kemp, T.A. Kung, C.A. Chestek, P.S. Cederna, A regenerative peripheral nerve interface allows real-time control of an artificial hand in upper limb amputees, Sci. Transl. Med. 4 (533) (2020) eaay2857, https://doi.org/10.1126/scitranslmed.aay2857.
[31] E.J. Earley, R.E. Johnson, J.W. Sensinger, L.J. Hargrove, Joint speed feedback improves myoelectric prosthesis adaptation after perturbed reaches in non amputees, Sci. Rep. 11 (1) (2021) 5158, https://doi.org/10.1038/s41598-021-84795-5.
[32] S. Pancholi, A.M. Joshi, Improved classification scheme using fused wavelet packet transform based features for intelligent myoelectric prostheses, IEEE Trans. Ind. Electron. 67 (10) (2020) 8517–8525, https://doi.org/10.1109/tie.2019.2946536.
[33] S. Huang, H. Huang, Voluntary control of residual antagonistic muscles in transtibial amputees: feedforward ballistic contractions and implications for direct neural control of powered lower limb prostheses, IEEE Trans. Neural Syst. Rehabil. Eng. 26 (4) (2018) 894–903, https://doi.org/10.1109/TNSRE.2018.2811544.
[34] M. Botvinick, C J, Rubber hands' feel' touch that eyes see, Nature (1998) 391, https://doi.org/10.1038/35784.
[35] M.R. Longo, P. Haggard, An implicit body representation underlying human position sense, Proc. Natl. Acad. Sci. U. S. A. 107 (26) (2010) 11727–11732, https://doi.org/10.1073/pnas.1003483107.
[36] C. Montell, Coordinated movement: watching proprioception unfold, Curr. Biol. 29 (6) (2019) R202–R205, https://doi.org/10.1016/j.cub.2019.02.004.
[37] V. Weerdesteyn, K.L. Hollands, M.A. Hollands, Gait adaptability, Handb. Clin. Neurol. 159 (2018) 135–146, https://doi.org/10.1016/B978-0-444-63916-5.00008-2.
[38] R.J. Peterka, Sensory integration for human balance control, Handb. Clin. Neurol. 159 (2018) 27–42, https://doi.org/10.1016/B978-0-444-63916-5.00002-1.
[39] R.J. Peterka, C.F. Murchison, L. Parrington, P.C. Fino, L.A. King, Implementation of a central sensorimotor integration test for characterization of human balance control during stance, Front. Neurol. 9 (2018) 1045, https://doi.org/10.3389/fneur.2018.01045.
[40] P.A. Forbes, A. Chen, J.S. Blouin, Sensorimotor control of standing balance, Handb. Clin. Neurol. 159 (2018) 61–83, https://doi.org/10.1016/B978-0-444-63916-5.00004-5.
[41] A. Mirelman, S. Shema, I. Maidan, J.M. Hausdorff, Gait, Handb. Clin. Neurol. 159 (2018) 119–134, https://doi.org/10.1016/B978-0-444-63916-5.00007-0.
[42] M.P. Mileusnic, I.E. Brown, N. Lan, G.E. Loeb, Mathematical models of proprioceptors. I. Control and transduction in the muscle spindle, J. Neurophysiol. 96 (4) (2006) 1772–1788, https://doi.org/10.1152/jn.00868.2005.
[43] J. Day, L.R. Bent, I. Birznieks, V.G. Macefield, A.G. Cresswell, Muscle spindles in human tibialis anterior encode muscle fascicle length changes, J. Neurophysiol. 117 (4) (2017) 1489–1498, https://doi.org/10.1152/jn.00374.2016.
[44] D. Wu, I. Schieren, Y. Qian, C. Zhang, T.M. Jessell, J.C. de Nooij, A role for sensory end organ-derived signals in regulating muscle spindle proprioceptor phenotype, J. Neurosci. 39 (22) (2019) 4252–4267, https://doi.org/10.1523/JNEUROSCI.2671-18.2019.
[45] C.D. MacKinnon, Sensorimotor anatomy of gait, balance, and falls, Handb. Clin. Neurol. 159 (2018) 3–26, https://doi.org/10.1016/B978-0-444-63916-5.00001-X.
[46] M.C.J. Seyedali, D.C. Morgenroth, M.E. Hahn, Co-contraction patterns of trans-tibial amputee ankle and knee musculature during gait, J. NeuroEng. Rehabil. 9 (2012) 29, https://doi.org/10.1186/1743-0003-9-29.
[47] T.R. Clites, M.J. Carty, J.B. Ullauri, M.E. Carney, L.M. Mooney, J.F. Duval, S.S. Srinivasan, H.M. Herr, Proprioception from a neurally controlled lower-extremity prosthesis, Sci. Transl. Med. 10 (443) (2018) eaap8373, https://doi.org/10.1126/scitranslmed.aap8373.
[48] S.S. Srinivasan, M. Diaz, M. Carty, H.M. Herr, Towards functional restoration for persons with limb amputation: a dual-stage implementation of regenerative agonist-antagonist myoneural interfaces, Sci. Rep. 9 (1) (2019) 1981, https://doi.org/10.1038/s41598-018-38096-z.
[49] T.R. Clites, M.J. Carty, S.S. Srinivasan, S.G. Talbot, R. Branemark, H.M. Herr, Caprine models of the agonist-antagonist myoneural interface implemented at the above- and below-knee amputation levels, Plast. Reconstr. Surg. 144 (2) (2019) 218e–229e, https://doi.org/10.1097/PRS.0000000000005864.
[50] S.S. Srinivasan, H.M. Herr, T.R. Clites, S. Gutierrez-Arango, A. Teng, L. Beltran, H. Song, E. Israel, M.J. Carty, Agonist-antagonist myoneural interfaces in above-knee amputation preserve distal joint function and perception, Ann. Surg. 273 (3) (2021) e115–e118, https://doi.org/10.1097/SLA.0000000000004153.
[51] P. Santos, T. Hortobagyi, I. Zijdewind, L.T. Bucken Gobbi, F.A. Barbieri, C. Lamoth, Minimal effects of age and prolonged physical and mental exercise on healthy adults' gait, Gait Posture 74 (2019) 205–211, https://doi.org/10.1016/j.gaitpost.2019.09.017.
[52] D. Renggli, C. Graf, N. Tachatos, N. Singh, M. Meboldt, W.R. Taylor, L. Stieglitz, Daners M. Schmid, Wearable inertial measurement units for assessing gait in real-world environments, Front. Physiol. 11 (2020) 90, https://doi.org/10.3389/fphys.2020.00090.
[53] J. Nonnekes, R.J.M. Goselink, E. Ruzicka, A. Fasano, J.G. Nutt, B.R. Bloem, Neurological disorders of gait, balance and posture: a sign-based approach, Nat. Rev. Neurol. 14 (3) (2018) 183–189, https://doi.org/10.1038/nrneurol.2017.178.